J. Physiol. (1974), **242**, *pp.* 321–351
With 12 text-figures
Printed in Great Britain

MOVEMENTS OF LABELLED SODIUM IONS IN ISOLATED RAT SUPERIOR CERVICAL GANGLIA

BY D. A. BROWN* AND C. N. SCHOLFIELD†

From the Department of Pharmacology, St Bartholomew's Hospital Medical College, Charterhouse Square, London, E.C. 1

(*Received 14 January 1974*)

SUMMARY

1. Isolated rat superior cervical ganglia were incubated in Krebs solution containing ^{24}Na and carbachol for 4 min at 25° C. They were then washed at 3° C for 15 min to remove extracellular ^{24}Na and the efflux of residual intracellular ^{24}Na stimulated by warming to 25° C.

2. During the 15 min wash at 3° C desaturation curves became exponential with a rate constant of $0{\cdot}012 \pm 0{\cdot}001$ min^{-1} ($n = 24$). This was assumed to represent loss of intracellular ^{24}Na, and initial uptake of ^{24}Na was calculated therefrom by back-extrapolation to zero wash-time. After 4 min in $^{24}Na + 180$ μM carbachol intracellular [^{24}Na] so calculated was $61{\cdot}6 \pm 3{\cdot}1$ mM ($n = 18$), representing 83% labelling of intracellular Na. In the absence of carbachol intracellular [^{24}Na] was $10{\cdot}0 \pm 0{\cdot}5$ mM, representing 49% labelling. Extracellular Na was labelled by > 90% after 4 min in ^{24}Na. The apparent rate constant for washout of extracellular ^{24}Na was 0·6 min^{-1} at 3° C and 0·95 min^{-1} at 25° C.

3. The loss of the residual intracellular ^{24}Na during temperature stimulation was interpreted quantitatively in terms of an exponential decline of the bulk of intracellular ^{24}Na with an extrusion rate constant of $0{\cdot}39 \pm 0{\cdot}1$ min^{-1} ($n = 18$), efflux being delayed by passage through the extracellular space with an effective rate constant of 0·8–1·2 min^{-1}.

4. The peak rate constant (k^C) for the desaturation curve at 25° C was $0{\cdot}35 \pm 0{\cdot}01$ min^{-1}. An Arrhenius plot of log $k^C/T° K^{-1}$ yielded a two-stage linear regression with a transition at 20° C. Activation energies of 8 and 31 kcal. mole^{-1} were calculated above and below this transition respectively.

5. Omission of K from the 25° C temperature-stimulating solution reduced k^C by 62%. The K-sensitive component of extrusion rate constant

* Present address: Department of Pharmacology, School of Pharmacy, University of London, 29/39 Brunswick Square, London WC1N 1AX.

† Present address: Department of Psychology, University of Iowa, Iowa City, Iowa 52242, U.S.A.

was a hyperbolic function of $[K]_e$ with half-saturation at 5·6 mM-$[K]_e$ and maximum k^C of 0·58 min^{-1}.

6. Cyanide (2 mM), 2,4-dinitrophenol (1 mM) and ouabain (1·4 mM) reduced k^C by 50–90 %. The half-maximally inhibiting concentration of ouabain was about 60 μM.

7. Substitution of sucrose, Li or choline for external Na did not reduce the extrusion rate of ^{24}Na in either 6 mM-$[K]_e$ or 0 mM-$[K]_e$. Li stimulated ^{24}Na extrusion in Na-free, K-free solution.

8. The properties of the ganglionic Na pump deduced from rates of temperature-stimulated ^{24}Na extrusion accord with the view that the ganglion hyperpolarization observed after Na loading by exposure to nicotinic depolarizing agents results from electrogenic Na extrusion. A comparable hyperpolarization is observed after temperature stimulation following Na loading.

INTRODUCTION

Exposure of isolated rat sympathetic ganglia for a few minutes to nicotinic depolarizing agents produces a large (up to 100 mM) rise in intracellular Na concentration (Brown & Scholfield, 1974). The subsequent extrusion of this accumulated Na is accompanied by ganglion cell hyperpolarization, apparently reflecting the electrogenic nature of the Na pump (Kosterlitz, Lees & Wallis, 1968, 1970; Brown, Brownstein & Scholfield, 1969, 1972). This electrogenic hyperpolarization provides a means of studying the properties of the ganglionic Na pump, but is rather indirect and the conclusions drawn therefrom depend critically upon certain assumptions regarding the proportionality between electrogenic and total Na extrusion, and between the Na current and the recorded hyperpolarization (Rang & Ritchie, 1968; Brown *et al.* 1972). In consequence, it seemed desirable to seek corroborative information in a more direct manner, by measuring the rate of Na-extrusion from ganglia loaded with ^{24}Na in the presence of a depolarizing agent.

METHODS

Superior cervical ganglia were dissected from urethane-anaesthetized rats (250–350 g. either sex). The connective tissue capsule was removed, the ganglion mounted on a stainless-steel wire frame and placed in normal Krebs solution at 25° C bubbled with 95 % O_2/5 % CO_2 gas mixture for at least 1 hr before experimentation. The composition of the Krebs solution (and of other solutions used in these experiments) were as described previously (Brown *et al.* 1972; Brown & Scholfield, 1974).

Ganglia were loaded with ^{24}Na by immersion at 25° C for (usually) 4 min in 1 ml. Krebs solution containing $^{24}NaCl$ at an initial activity of up to 1 $mC.ml.^{-1}$ (specific activity up to 7 $mC.m\text{-}mole^{-1}$). The ^{24}Na was received from the Radiochemical Centre, Amersham, as an 'isotonic' NaCl solution (about 150 mM) of specific activity

up to 8 mC.m-mole^{-1}: other ions were added as 0·1 ml. of a concentrated solution to 0·9 ml. ^{24}NaCl, to attain the composition of normal Krebs solution.

After loading, the ganglion was rinsed briefly (3 sec) in non-radioactive Krebs solution. Subsequent efflux of ^{24}Na was then monitored by transferring the ganglion at (usually) 1 min intervals through a series of vials containing 12 ml. non-radioactive Krebs solution, with 2·5 mM hexamethonium added to arrest any residual effect of carbachol on passive Na permeability (Brown *et al.* 1972). The radioactivity collected in each vial was measured in a liquid scintillation counter by Cerenkov emission, at an efficiency of about 20 %. At the end of the efflux period the radioactivity remaining in the ganglion (still immersed in Krebs solution) was similarly counted so that the total amount of radioactivity in the ganglion at any preceding time t could be calculated by adding the radioactivity lost after time t to that remaining at the end of the experiment. The radioactivity in the loading solutions were also measured, to determine the specific activity of the ^{24}Na solution. All counts were corrected for radioactive decay. At the end of the experiment, when all ^{24}Na had been washed out, extracellular (Li) space, wet-weight and water content were determined as described previously (Brown & Scholfield, 1974). From this data, extracellular and intracellular fluid volumes could be calculated and intracellular radioactivity (deduced from the efflux curves, see below) expressed as m-moles (kg cell water)$^{-1}$ ^{24}Na, at the specific activity of the external medium.

Several load-and-efflux 'runs' were completed on each preparation at intervals of not less than 40 min over a period of up to 10 hr. The duration of the experiment was limited more by the decline in ^{24}Na activity than by deterioration of the ganglion. Thus, in a number of preparations the Na and K contents of the tissue were measured by flame photometry (Brown & Scholfield, 1974) after the last tracer run had been completed. Intracellular ion concentrations were (m-mole (kg cell water)$^{-1}$): Na, 23·5 ± 2·7, and K, 195 ± 6·1 (means ± S.E. of means, fifteen ganglia). These compare well with those measured in freshly incubated ganglia (Na, 19·8 ± 0·9, and K, 192·7 ± 2·8 m-moles (kg cell water)$^{-1}$; Brown & Scholfield, 1974).

Analytical procedures

(1) *Expression of count data*

At its simplest (see Brown *et al.* 1972) the rate at which Na is extruded from ganglion cells might be a first-order function of the intracellular Na concentration. Then the amount of intracellular ^{24}Na (a) and its rate of efflux (m) might both diminish exponentially with time (t) according to the expressions

$$a_t = a_0 \exp(-k_a t) \tag{1}$$

and

$$m_t = k_a a_0 \exp(-k_a t), \tag{2}$$

where a_t and m_t are the intracellular ^{24}Na contents and efflux rates respectively after time t, a_0 is the initial amount of intracellular ^{24}Na at $t = 0$, and k_a is the rate constant for Na-extrusion. Expressing both content and efflux rate as a fraction of the initial intracellular content and taking logarithms:

$$\log\left(\frac{a_t}{a_0}\right) = \frac{-k_a}{2{\cdot}303}.t \tag{3}$$

and

$$\log\left(\frac{m_t}{a_0}\right) = \frac{-k_a}{2{\cdot}303}.t + \log k_a. \tag{4}$$

Fractional ^{24}Na contents and efflux rates corresponding to a_t/a_0 and m_t/a_0 were calculated from the count data and plotted on a logarithmic scale against time, to

give curves which we refer to as *desaturation* and *efflux* curves respectively. Eqs. (3) and (4) suggest that these curves would be linear and parallel with slopes equal to $-k_a/2{\cdot}303$, but displaced along the ordinates by an amount log k_a. The rate constant k_a can then be obtained from the slope of either curve. In practice, the two curves were not parallel (see section (3) below): hence two rate constants could be measured – k^C for the desaturation ('contents') curve and k^E for the efflux curve. The rate constant k^C was more conveniently measured directly from the count data, by dividing the effluent radioactivity collected over a 1 min period by the arithmetic mean of the tissue radioactivity measured at the beginning and end of the same collection period. This calculated rate constant approximates to that which would be obtained by dividing eqn. (2) by eqn. (1). Because finite time intervals and arithmetic means were used, it underestimates the true value of k^C by (maximally) 5% at the extrusion rates encountered in the present experiments. These calculated values of k^C were plotted against time as shown in Figs. 2*b* and 7*b*, a continuous curve drawn through the points, and the maximum value derived therefrom used as a practical measure of the Na extrusion rate constant.

(2) *Experimental separation of intracellular and extracellular sources of effluent ^{24}Na*

Freshly loaded ganglia contain ^{24}Na in both intracellular and extracellular fluids so that the effluent radioactivity measured immediately after loading is derived from both sources. Resolution of the efflux curves into its two components source by graphical means is then difficult because the two compartments are essentially 'in series' and the rate constants for exit from the two compartments are rather close (cf. Huxley, 1960; Brinley, 1963).

To overcome this difficulty, the two sources of effluent ^{24}Na were separated temporally by varying the temperature of the surrounding medium in the manner shown in Fig. 1. Immediately after loading, the ganglion was immersed in non-radioactive solution at 3° C to retard the egress of intracellular ^{24}Na and allow the ^{24}Na accumulated in the extracellular fluid to escape. Removal of extracellular ^{24}Na was judged complete by the assumption of a single exponential in the desaturation curve with a rate constant of around 0·01 min^{-1} (see above, equation (1)). A wash time of 15 min was normally sufficient for this. The ganglion was then transferred to Krebs solution at 25° C to stimulate the Na pump and the subsequent efflux of the residual intracellular ^{24}Na monitored. Following temperature-elevation the desaturation curve tended to a new exponential with (in Fig. 1) a rate constant of 0·39 min^{-1}. This method of isolating intracellular ^{24}Na we refer to hereafter as '*temperature-stimulation*'.

A comparable experimental technique for studying Na-extrusion from other tissues was reported during our experiments by Bittar (1971) and Bosteels & Carmeliet (1972). It has the advantage that the inhibition of Na-extrusion by cooling is sufficiently great as to conserve most (about 84%, see below) of the intracellular ^{24}Na originally present. We tried other forms of inhibition and reactivation (such as K-activation, cf. Rang & Ritchie, 1968), but the inhibition in (e.g.) K-free solution was less complete and reactivation on replacing K less rapid. As far as we could ascertain, cooling had no deleterious effect on the subsequent temperature-stimulated extrusion of Na: the rate constant for temperature-stimulated ^{24}Na efflux was no less than that provoked by replacing K, and the electrogenic effect was comparable to that observed previously immediately after washing out the carbachol (see Fig. 7).

(3) *Kinetics of temperature-stimulated ^{24}Na exit*

Experimental curves for the loss of residual intracellular ^{24}Na during temperature-stimulation were not simple exponentials as predicted in eqs. (1) and (2). Fig. 2 illustrates such curves from an experiment where ^{24}Na of high specific activity was used: this was particularly helpful for kinetic analysis since the effluent count rate was high enough to allow measurements over some seven time constants (18 min) as opposed to the more usual four time constants elapsing before the count rate fell below measurable values (as in the mean curves of Fig. 7). Two clear deviations from the predicted exponentials are seen. Firstly, the efflux of ^{24}Na is delayed, so

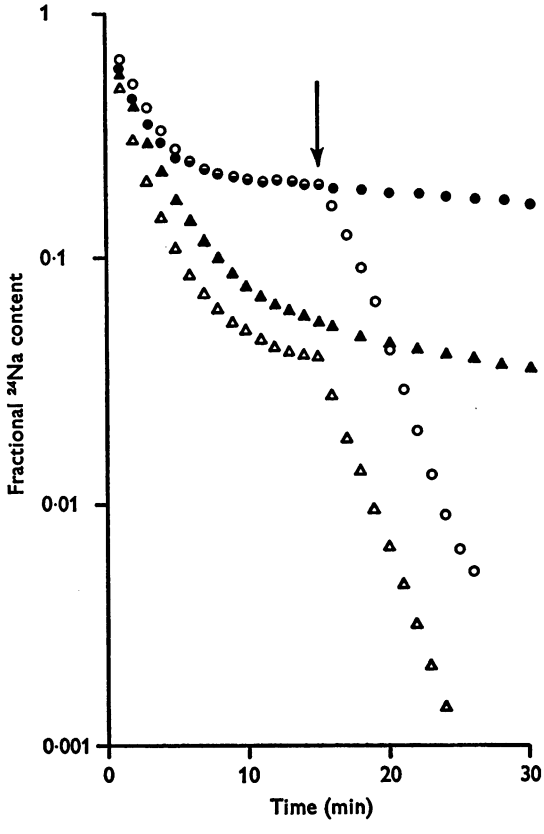

Fig. 1. Decline of ^{24}Na content in two ganglia (represented separately by the open and filled symbols, respectively) on washing in normal Krebs solution at 3° C. Each ganglion was loaded for 4 min at 25°C in ^{24}Na solution twice, in the absence (△, ▲) and presence (○, ●) of 180 μM carbachol, before commencing efflux measurements. One ganglion (●, ▲) was then washed continuously at 3° C; the other (○, △) was warmed to 25° C after washing for 15 min at 3° C (at arrow). ^{24}Na content (ordinates) is expressed as the fraction of ^{24}Na present in the tissue after loading, and is calculated by adding the radioactivity released into the collecting medium to that present in the tissue at the end of the efflux run (see Methods).

that the maximum *rate* of efflux occurs in the second minute after warming rather than instantaneously, and the peak *rate constant* (Fig. 2*b*) is not attained until the sixth minute. Secondly, the slope of the desaturation curve, and hence the rate constant k^C, diminished strongly after 10 min without any corresponding diminution in the slope of the efflux curve and hence rate constant k^E (see section (1) above). Probable causes of these effects are (*a*) delays in the appearance of effluent intracellular ^{24}Na in the surrounding medium incurred through passage through the extracellular space; and (*b*) an inhomogeneous distribution of intracellular ^{24}Na within the tissue. These factors, and their influence on the measurement of Na extrusion, are examined further below using the experimental data in Fig. 2 as a guide for quantitative predictions.

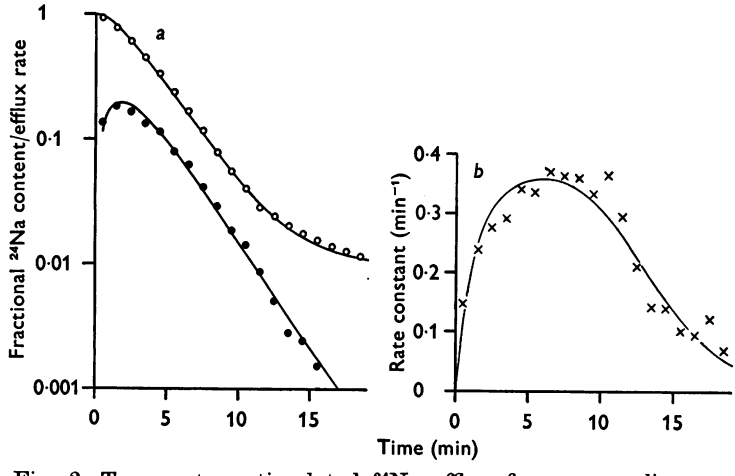

Fig. 2. Temperature-stimulated ^{24}Na efflux from a ganglion previously loaded for 4 min in ^{24}Na solution, washed at 3° C for 15 min and then warmed to 25 °C to stimulate ^{24}Na extrusion as in Fig. 1. Time (abscissa) reads from the time of warming. In *a* points show tissue ^{24}Na content (○) and ^{24}Na efflux rate (●), both expressed as a fraction of the ^{24}Na remaining in the tissue after the 15 min cold wash (as in text-eqns. (3) and (4)). In *b* the calculated rate constant k^C (=mean efflux rate/arithmetic mean tissue ^{24}Na content, see Methods) during each 1 min collection period is plotted against time. Smooth curves are constructed from text-eqns. (7) and (8) for two summed intracellular compartments (text-eqns. (11) and (12)), using constants given in the text p. 328.

(*a*) *Transit through extracellular space.* If the cells, extracellular space and collecting fluid are considered as three compartments (*A*, *B* and *C*) in series containing amounts of radioactivity *a*, *b* and *c*, the *measured* amount of radioactivity in the tissue (*y*) at any time *t* is

$$y_t = a_t + b_t. \tag{5}$$

After 15 min washing at 3° C, when $t = 0$, extracellular radioactivity is nil (i.e. $b_0 = 0$), so that the initial radioactivity is entirely intracellular and $y_0 = a_0$ in eqn. (1). At any time thereafter there might be present in the extracellular space a finite amount of radioactivity given by (Teorell, 1937; Atkins, 1969):

$$b_t = \frac{k_a a_0}{k_b - k_a}[\exp(-k_a t) - \exp(-k_b t)], \tag{6}$$

where k_a and k_b are rate constants for exit of radioactivity from the intracellular and extracellular compartments respectively, and $k_a \neq k_b$. (This assumes an unidirectional flow of radioactivity in the direction $A \rightarrow B \rightarrow C$ governed by single rate constants).

Then, the *total tissue content* y_t at any time $t \neq 0$ is given by substituting (1) and (6) in (5) as

$$y_t = a_0 \exp(-k_a t) + \frac{k_a a_0}{k_b - k_a}[\exp(-k_a t) - \exp(-k_b t)]. \quad (7)$$

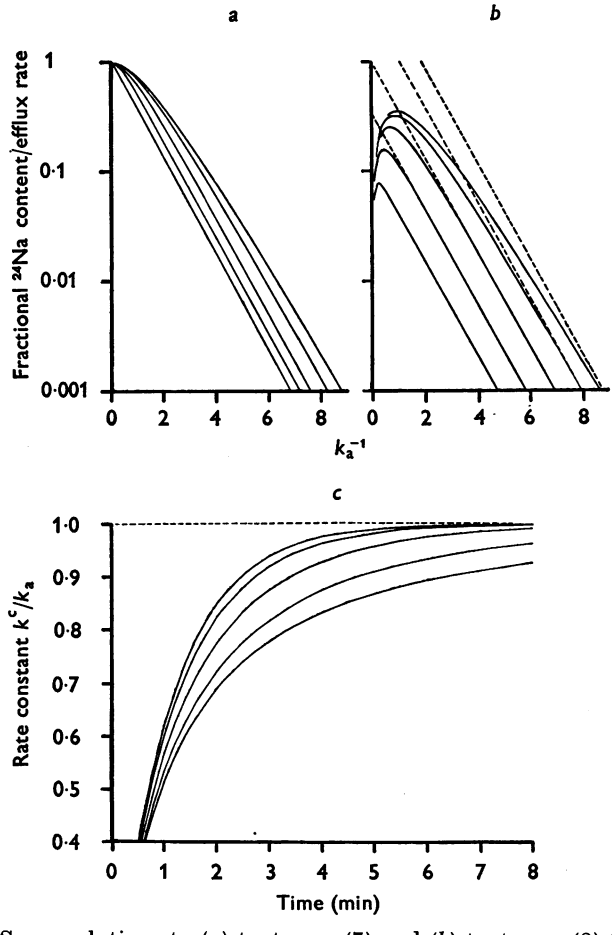

Fig. 3. Some solutions to (*a*) text-eqn. (7) and (*b*) text-eqn. (8) for values of k_a/k_b (intracellular:extracellular rate constants) of 0·1, 0·25, 0·5, 0·75 and 0·9. Ordinates: (*a*), apparent (observed) ^{24}Na content of the tissue (i.e. sum of intracellular and extracellular contents), and (*b*) apparent (observed) efflux rate into the collecting medium, both expressed as a fraction of the initial ^{24}Na content. Abscissae: efflux time, in time constants ($=k_a^{-1}$). In (*c*) the apparent rate constant k^c, obtained by dividing (*a*) by (*b*), is expressed as a fraction of k_a for values of $k_a = 0{\cdot}1$, 0·25, 0·5, 0·75 and 0·9 min^{-1}, and plotted against real efflux time in min, taking $k_b = 1$ min^{-1}.

The measured efflux rate is the rate of appearance of radioactivity in compartment C and is given by $M = dc/dt = k_b b$, whence, from (6):

$$M = k_b \cdot \frac{k_a a_0}{k_b - k_a} \cdot [\exp(-k_a t) - \exp(-k_b t)]. \quad (8)$$

Some general solutions to eqns. (7) and (8) using different ratios for the intracellular and extracellular rate constants ($k_a : k_b$) between 0·1 and 0·9 are shown in Fig. 3*a* and *b*. Comparing with the situation where ^{24}Na passes directly from the cells into the collecting medium, as represented by eqns. (1) and (2), interpolation of an extracellular space produces the following alterations to the curves.

(i) The *time* at which the peak rate of efflux is attained is increased from zero (as per eqn. 2) to a finite time given (by differentiating (8), setting $dM/dt = 0$ and taking logarithms) as:

$$t_{max} = \frac{2{\cdot}303}{k_b - k_a} \log \frac{k_b}{k_a}. \quad (9)$$

(ii) The maximum efflux *rate* is reduced from $m_{max} = k_a a_0$ (eqn. (2)) to:

$$M_{max} = a_0 k_b \left[\frac{k_a}{k_b}\right]^{(k_b(k_b - k_a)^{-1})} \quad (10)$$

(iii) The apparent *rate constant* given by the slope of the semilogarithmic curves in Fig. 3 under-reads k_a by an amount which diminishes asymptotically with increasing efflux duration. Thus, the accuracy with which k_a can be estimated from the slope of the experimental curves will depend both upon the time at which it is measured and the ratio $k_a : k_b$. This is shown in Fig. 3*c*. Here we have assumed a fixed value for the extracellular rate constant k_b of 1 min^{-1} at 25 °C (see Table 1; compatible values are given by Harris & McLennan, 1953; and Brinley, 1967), and have calculated the ratio of the rate constant k^C measured from the slope of the curves in Fig. 3*a* to the true rate constant k_a after increasing efflux times for various values of k_a. From the present and previous experiments (cf. Brown *et al.* 1972) we estimate that k_a usually lies between 0·3 and 0·5 min^{-1} during vigorous Na-pumping and the peak slope of the experimental curve, from which the experimental rate constant k^C was determined (see (1) above), is usually attained between 5 and 10 min after washing. Reference to Fig. 3*c* suggests that, under these conditions, the measured rate constant should not underestimate k_a by more than 5 %.

(*b*) *Sub-compartments of intracellular* ^{24}*Na*. The reducing rate constant after some 10 min washing, and the divergence of the integrated and differentiated curves in Fig. 2 could be explained if the intracellular ^{24}Na were distributed between a number of parallel separate intracellular compartments with differing rate constants, each feeding independently into the extracellular space (Persoff, 1960). For example, taking two intracellular compartments $A_{(1)}$ and $A_{(2)}$ containing amounts of ^{24}Na $a_{t(1)}$, $a_{t(2)}$ respectively at time t, the total amount of intracellular ^{24}Na at time t is

$$a_t = a_{t(1)} + a_{t(2)}$$

whence, from eqn. (1):

$$a_t = a_{0(1)} \exp(-k_{a(1)} t) + a_{0(2)} \exp(-k_{a(2)} t), \quad (11)$$

where $k_{a(1)}$ and $k_{a(2)}$ are the rate constants for exit from $A_{(1)}$ and $A_{(2)}$ respectively. The over-all rate of efflux into the extracellular space from eqn. (2) is:

$$m_t = k_{a(1)} a_{0(1)} \exp(-k_{a(1)} t) + k_{a(2)} a_{0(2)} \exp(-k_{a(2)} t) \quad (12)$$

A reasonable trial fit to the experimental data in Fig. 2 (continuous curve) could be obtained using eqns. (11) and (12) with, as constants, $a_{0(1)} = 0{\cdot}9885$, $a_{0(2)} =$

0·0115 ($a_{0(1)}+a_{0(2)}=1$), $k_{a(1)}=0{\cdot}4$ min^{-1} and $k_{a(2)}=0{\cdot}01$ min^{-1} (the summed data being substituted in eqns. (7) and (8) setting $k_a=0{\cdot}83$ min^{-1}). Solution was simplified by the fact that the second term in eqn. (12) rapidly becomes negligible, so that the maximum rate constant for the differentiated efflux curve (k^E) is equal to $k_{a(1)}$. On the other hand the rate constant k^C for the desaturation curve is a composite rate constant attaining, at its maximum, 0·9 $k_{a(1)}$ and reducing to $k_{a(2)}$ at $t=\infty$.

The anatomical basis for these apparently separate pools of intracellular ^{24}Na is not clear (see Appendix). Consequently, there is no compelling reason for supposing one or other rate constant as the better index of Na extrusion. As pointed out in (1) above, we have used the maximum value of k^C, calculated directly from the count data, as the most convenient measure for comparative purposes. Overall, $k^C{}_{max}$ was about 10 % less than k^E at 25° C (Table 1), and, as indicated previously, might otherwise underestimate k_a by up to 10 % on other grounds.

(4) *Uptake of ^{24}Na during loading*

The amount of ^{24}Na accumulated intracellularly during the loading procedure was determined by extrapolating the slow exponential component of the 3° C desaturation curve to zero time, and the initial extracellular ^{24}Na was calculated by subtracting this value from the total initial tissue radioactivity. This graphical procedure is feasible, notwithstanding the sequential nature of the two compartments, because the rate constants for exit of intracellular and extracellular ^{24}Na differ by 50-fold at 3° C (Fig. 1): in consequence, negligible (< 1 %) error results in translating directly from graphical components to physical compartments (see eqn. (B8) of Huxley, 1960).

It may be noted that, in the prototype experiment illustrated in Fig. 1, this extrapolation yielded values of 1·1 and $4{\cdot}4\times10^4$ c.p.m. for the initial size of the slow-efflux compartment after loading the ganglion in the absence and presence of carbachol respectively. Subtraction from total counts gave values of 20·8 and 19·9 c.p.m. for the fast-efflux compartment in these two situations. Assuming the effect of carbachol to be solely to increase intracellular ^{24}Na, these values accord with the view that the slow and fast components observed at 3° C reflect losses of intra- and extracellular ^{24}Na respectively, and thereby substantiate the conclusion that the extracellular ^{24}Na is effectively cleared after 15 min at this temperature. The amount of 'extracellular' ^{24}Na measured in this way exceeds that appropriate to the extracellular space since it includes adhering ^{24}Na solution. In determining the extracellular ^{24}Na space, a correction for adhering ^{24}Na was made using losses from cotton thread as a 'blank': the amount of adhering ^{24}Na corresponded to that in 0·03 μl. of loading solution, loss of which was complete after 1 min washing.

In experiments where only the uptake of *intracellular* ^{24}Na was required, graphical extrapolation was replaced by a calculated extrapolation based on eqn. (1). The residual radioactivity in the tissue after 15 min washing at 3° C was measured and assumed to be entirely intracellular. This value was substituted as a_t in eqn. (1) and initial intracellular radioactivity a_0 calculated taking an average value of 0·012 min^{-1} for the rate constant k_a at 3 °C (Results). This gives $a_t/a_0=0{\cdot}835$, i.e. 16·5 % of the initial intracellular radioactivity was lost after 15 min at 3 °C. Radioactivity was converted to concentration using intracellular spaces as described above. This procedure permitted repeated estimates of ^{24}Na uptake in a single preparation.

(5) *Extracellular washout*

Washout of ^{24}Na from the extracellular space could be followed at 3 °C by subtracting the slow exponential component of intracellular ^{24}Na loss from total tissue content with minimal error as described in (4) above. Estimation of extracellular

washout rates at 25° C by graphical methods was more difficult because the efflux curve could not be resolved visually into intracellular and extracellular components. Some attempts at graphical resolution of extracellular efflux at 25° C were made by loading ganglia with ^{24}Na in the absence of carbachol (to minimize intracellular labelling) and subtracting a calculated intracellular component from the subsequent 25° C efflux curve using the mean data from observations on temperature-stimulated intracellular ^{24}Na efflux. In this we assumed the initial intracellular ^{24}Na to be 7 % of total tissue ^{24}Na (corresponding to 10 mM intracellular [^{24}Na] after 4 min loading, of Fig. 4) and the rate constant k_a for loss of intracellular ^{24}Na to be 0·35 min^{-1} (Table 1). If the true rate constant for extracellular clearance k_b were (minimally) 0·7 min^{-1} (Table 1), eqn. (14) of Brinley (1963) predicts that the apparent rate constant for the residual fast-clearing component would over-estimate k_b by $\leqslant$ 10 %.

Approximate values for k_b at 25° C were also calculated from the measured efflux after temperature stimulation assuming the effect of the extracellular space on the desaturation and efflux curves to be that depicted in Fig. 3. Two calculations were made: (*i*) from the observed peak efflux rate, by substituting $k_a = k^E$ in eqn. (10) and solving by trial-and-error; and (*ii*) from the vertical displacement of the observed desaturation curve in Fig. 3*a* at time *t* from that predicted in the absence of an extracellular space. If time *t* is sufficiently large that $\exp(-k_b t)$ in eqn. (7) tends to zero, (i.e. the log y/t curve is linear and parallel to the log a/t curve), then dividing equation (1) into eqn. (7) gives

$$k_b = k_a \frac{y_t}{a_t - y_t} \tag{13}$$

from which k_b can be calculated by substituting k^C for k_a. Slightly different values for k_b were obtained from eqns. (10) and (13), probably reflecting experimental inaccuracies and oversimplification in deriving eqn. (13) (for example, homogeneity of intracellular ^{24}Na is assumed, cf. (*b*) above).

RESULTS

Uptake of ^{24}Na

Extracellular accumulation

The extracellular fluid appeared to equilibrate fairly completely (> 90 %) with external ^{24}Na after the usual 4 min loading period. The mean extracellular ^{24}Na space, determined graphically from the subsequent efflux at 3° C as described in Methods, was 0·97 ± 0·10 times the extracellular (Li) space measured in the same tissues (mean ± S.E. of means of ten ganglia). Rapid equilibration may also be inferred from subsequent losses on washing: the fast-clearing component fell by 88 % at 3° C and by about 96 % at 25° C after 4 min washing (Fig. 6 below).

Intracellular accumulation

Cellular uptake of ^{24}Na, determined from subsequent 3° C efflux curves, was maximal after 30 min incubation with ^{24}Na at 25° C, both in the absence and presence of carbachol (Fig. 4). Uptake after 4 min was about 50–80 % of that after 30 min.

In the absence of carbachol the intracellular ^{24}Na concentration

($[^{24}Na]_i$) at 30 min was 14–15 mM (expressed at the specific activity of that in the external solution) compared with a total intracellular Na concentration ($[Na]_i$) of 23·5 mM measured by flame photometry (see Methods): therefore 60–70 % of intracellular Na appeared to be labelled.

Incubation in carbachol solution enhanced both uptake and labelling. After 4 min exposure to ^{24}Na in 180 μM carbachol $[^{24}Na]_i$ was 61·6 ± 3·1 mM

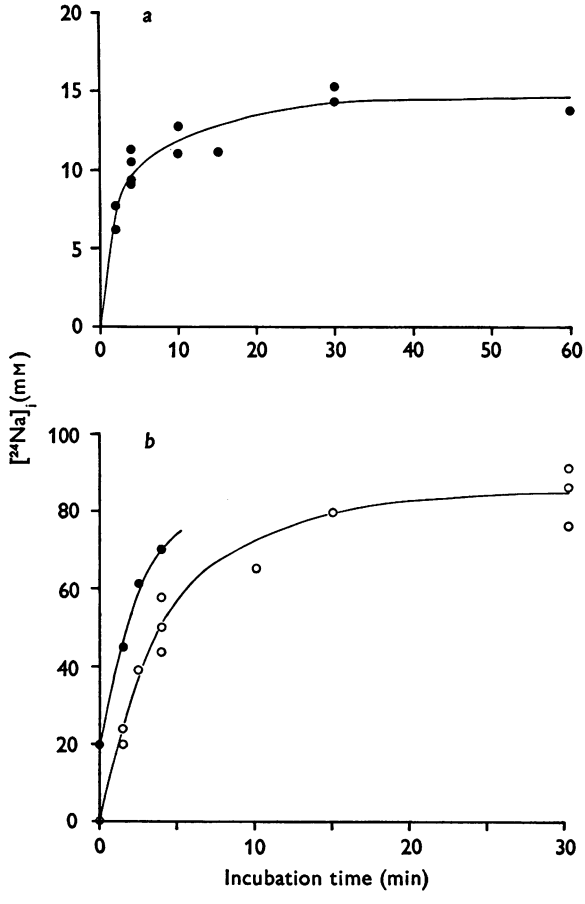

Fig. 4. Uptake of ^{24}Na: intracellular ^{24}Na concentrations (ordinates, m-moles ^{24}Na (kg cell fluid)$^{-1}$) after immersion for different times (abscissa, min) in ^{24}Na solution (*a*) without added carbachol and (*b*) containing 180 μM carbachol (filled circles in *b* are transposed from Fig. 2 of Brown & Scholfield (1974), and show total intracellular Na concentrations as measured by flame photometry). The intracellular ^{24}Na concentrations were calculated by extrapolating efflux curves measured at 3° C immediately after loading back to zero wash time, and are expressed at the specific activity of the loading solution (see Methods). Each point represents a single load-and-efflux measurement; points are taken from experiments on three ganglia for *a* and two ganglia for *b*.

(mean ± S.E. of mean of eighteen ganglia, Table 1). Total $[Na]_i$ measured previously under these conditions was 74·6 mM (Brown & Scholfield, 1974), suggesting about 83% labelling on average. Total $[Na]_i$ after longer exposures to carbachol has not been measured. Uptake of ^{24}Na increased with increasing concentrations of carbachol in the ^{24}Na-loading solution (using 4 min exposure periods) approximately in parallel with the increase in total $[Na]_i$ (Fig. 5; cf. Fig. 1 in Brown & Scholfield, 1974). The degree

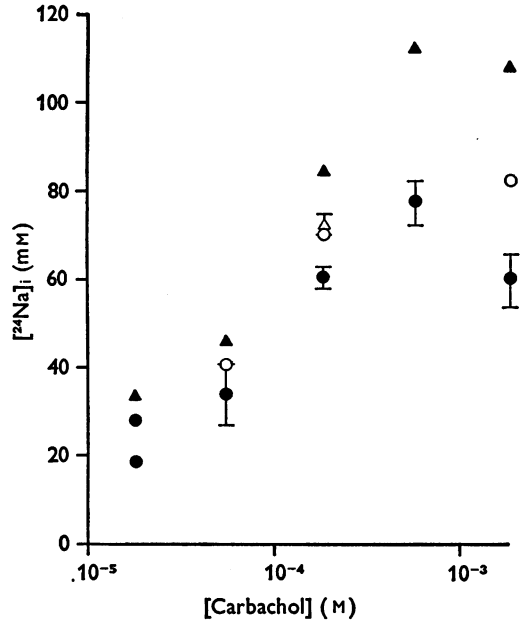

Fig. 5. Intracellular ^{24}Na concentrations (●) (ordinates, m-mole (kg cell fluid)$^{-1}$) in ganglia loaded for 4 min in ^{24}Na containing different concentrations of carbachol (abscissa, mM). ^{24}Na concentrations were determined from extrapolated cold-efflux measurements (see Methods). Each point (●) represents the mean of three to six determinations in six ganglia (except at 18 μM carbachol, which give single measurements); bars give S.E. of means. Open circles (○) show the results of single determinations when the ganglion was pre-incubated for 30 min in carbachol-free ^{24}Na solution before adding carbachol. Triangles show total intracellular Na concentrations measured in separate ganglia by flame photometry, and are transposed from data of Brown & Scholfield (1974).

to which intracellular Na was labelled appeared fairly constant, at 70–75% in these experiments. Labelling was increased (in one preparation) by ~ 15% on soaking the ganglion in ^{24}Na solution for 30 min before adding carbachol: this procedure was not routinely adopted, since it was inconvenient and labelling appeared otherwise adequate.

Washout of extracellular ^{24}Na

Ganglia were incubated for 4 min in ^{24}Na solution without added carbachol (to minimize intracellular labelling) and efflux curves for the subsequent loss of extracellular ^{24}Na at 3° C and 25° C constructed by graphical subtraction of an observed or calculated intracellular component as described in Methods. Averaged curves for the decline in the residual fast-clearing component of ganglionic ^{24}Na are shown in Fig. 6. As befits a bulk diffusion process, the curves were not simple exponentials but approached single exponentials after some 2–3 time constants. The initial

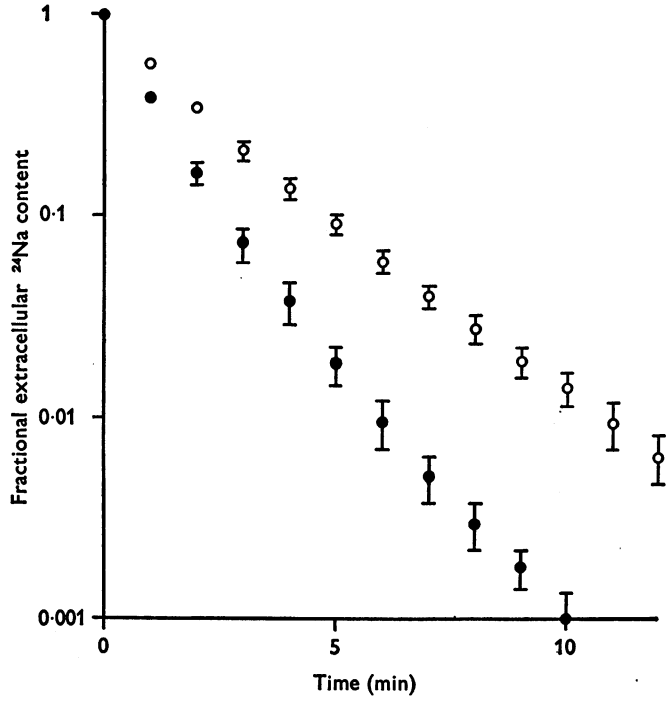

Fig. 6. Estimated rates of extracellular ^{24}Na loss at 3° C (○) and 25° C (●) after loading ganglia with ^{24}Na for 4 min in the absence of carbachol. Points were derived by subtracting intracellular efflux components from the averaged total ^{24}Na efflux in five ganglia at 25° C and from individual efflux curves from seven ganglia at 3° C; bars show S.E. of means (constants for the subtracted intracellular components used in this analysis were: $k_a = 0{\cdot}012$ (3° C) and 0·39 (25° C) min^{-1}; $a_0 = 0{\cdot}072$ (= 10 mM intracellular ^{24}Na, see Fig. 4*a*)).

slopes yielded maximum rate constants of 0·57 and 0·95 min^{-1} at 3° C and 25° C respectively. The former is probably an accurate measure of extracellular clearance rates but the latter probably overestimates the rate

constant for extracellular clearance by some 8% (see Methods). After correction, the apparent Q_{10} is 1·21. Calculations from eqns. (10) and (13) of the apparent rate constant k_b for transit of intracellular ^{24}Na across the extracellular space during temperature-stimulation (see below, Table 1) gave compatible values for k_b of 0·8–1·2 min^{-1} at 25° C.

An effective diffusion coefficient D ($cm^2.sec^{-1}$) for movement of ^{24}Na through the extracellular space may be calculated from Fig. 6, using Fig. 2.1. of Harris (1972) as a guide, and taking the ganglion as intermediate between a sphere and a cylinder with average radius 200 μm, D is then 6×10^{-7} $cm^2.sec^{-1}$. Harris & McLennan (1953) deduced a lower value of $0{\cdot}6–1{\cdot}0 \times 10^{-7}$ at 17° C but did not include a correction for intracellular efflux components. Taking the diffusion coefficient of 0·1 M-NaCl in free aqueous solution as $1{\cdot}6 \times 10^{-5}$ $cm^2.sec^{-1}$ at 25° C (Weast, 1971), the equivalent path for Na movement through the extracellular space appears to be about five times the actual radius of the ganglion.

Temperature-stimulated efflux of intracellular ^{24}Na

Efflux of intracellular ^{24}Na following temperature-stimulation at 25° C after 15 min washing at 3° C was monitored in the manner illustrated in Fig. 1. Fig. 7 shows mean desaturation and efflux curves from eighteen ganglia loaded with ^{24}Na by 4 min immersion in ^{24}Na solution containing 180 μM carbachol. Radioactivity was normalized by expressing all counts as a fraction of the residual radioactivity in the tissue remaining after 15 min washing at 3° C. The calculated rate constant k^C (Fig. 7*b*) attained a maximum value of 0·34 min^{-1} after 7 min, and declined after 10 min, reflecting the diminishing slope of the desaturation curve in Fig. 7*a*. This effect is discussed in Methods in connection with Fig. 2. The efflux curve remained exponential to 10 min, with a maximum efflux rate constant k^E of 0·36 min^{-1}.

In previous experiments (Brown *et al.* 1972) the electrogenic effect was monitored immediately after washing out the carbachol with Krebs solution at 25° C, without an intervening cold wash, although a temperature-stimulated hyperpolarization was observed in some experiments (see Fig. 5*a* in Brown *et al.* 1972). Temperature-stimulated hyperpolarization at 25° C following post-carbachol cooling to 3° C was verified in four ganglia during the course of the present experiments, and its time course is superimposed on the ^{24}Na efflux curves in Fig. 7*a*. The magnitude of the electrogenic contribution toward the initial hyperpolarization is uncertain because the resting membrane potential is also under the influence of concurrent changes in $[K]_I$ and in membrane conductance, but the time course of the later part of the temperature-stimulated hyperpolarization corresponds fairly well with that for ^{24}Na extrusion, with a rate constant of about 0·36 min^{-1}.

Some data calculated from these experiments is given in Table 1. The

mean maximum calculated rate constant k^C at 25° C from all 'runs' in normal Krebs solution at 25° C was $0{\cdot}35 \pm 0{\cdot}010$ min^{-1} compared with a mean maximum rate constant k^E deduced from the slopes of the efflux curves of $0{\cdot}39 \pm 0{\cdot}013$ min^{-1}. Taking the former as representing the rate constant for cellular extrusion k_a, and with a mean value of 54·6 mM as the intracellular ^{24}Na concentration prior to temperature stimulation the predicted maximal rate of loss of intracellular ^{24}Na according to equation

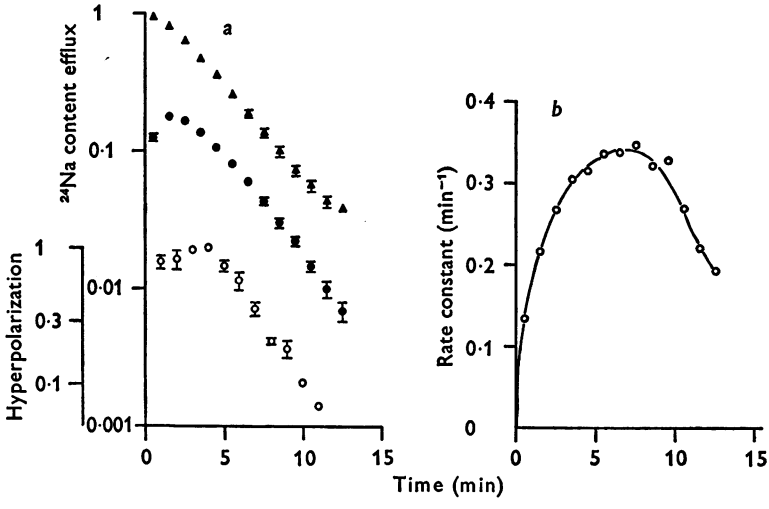

Fig. 7. Mean curves for 'temperature-stimulated' ^{24}Na efflux obtained from eighteen ganglia. Each ganglion was loaded for 4 min in ^{24}Na solution containing 180 μM carbachol, washed for 15 min at 3° C and then warmed to 25° C: observations refer to times after warming. Graphs in *a* show the tissue ^{24}Na content (▲) and the ^{24}Na efflux rate (●), each expressed as a fraction of the ^{24}Na remaining in the tissue after the cold wash (see Fig. 2). Graph *b* shows the mean calculated rate constant k^C for each minute collection period. The lower curve (○) in (*a*) shows the mean surface hyperpolarization (recorded separately in four ganglia in the manner described in Brown *et al.* 1972) on warming to 25° C after previous exposure to 180 μM carbachol for 4 min and washing at 3° C for 15 min, hyperpolarization at each time point being expressed as a fraction of the maximum attained. Bars show S.E. of means, where greater than the size of the points.

(1) would be 19·1 m-mole min^{-1} (corresponding to 23 m-mole min^{-1} total Na at 83 % labelling). As pointed out in Methods (eqn. (10)) the observed maximum efflux rate ($10{\cdot}4 \pm 0{\cdot}55$ m-mole min^{-1}) is less than the peak rate of cellular extrusion, because of delay imposed by the extracellular space.

Effect of temperature

The mean rate constant k^C before warming (i.e. after 15 min at 3° C) was $0{\cdot}012 \pm 0{\cdot}001$ min^{-1} (mean ± S.E.; twenty-four ganglia). Thus ^{24}Na extrusion was accelerated 28 times on warming from 3 to 25 °C. Effects of warming to other temperatures were measured in a series of five ganglia. In each of these experiments several 'runs' at different activation temperatures were completed, and the maximum rate constant k^C attained expressed as a fraction of that at 25° C in the same preparation, in order

TABLE 1. Summary of observations on ^{24}Na efflux from isolated rat superior cervical ganglia measured at 25° C. The ganglia were loaded for 4 min in ^{24}Na solution containing 180 μM carbachol, washed for 15 min at 3° C and efflux rates measured on subsequent warming to 25° C

Parameter	No. of ganglia	No. of 'runs'	Mean ± S.E. of mean
(1) Ganglion wet weight (mg)	15	—	1·25 ± 0·066
(2) Intracellular volume (μl.)	15	—	0·514 ± 0·028
(3) Intracellular [^{24}Na] after washing for 15 min at 3° C (m-mole (kg cell fluid)$^{-1}$)	15	31	54·6 ± 2·7
(4) Intracellular [^{24}Na] after loading (m-mole (kg cell fluid)$^{-1}$) (calculated from (3) by extrapolation)	15	31	61·6 ± 3·1
(5) Maximum rate constant k^C (min^{-1})	18	34	0·352 ± 0·010
(6) Maximum rate constant k^E (min^{-1})	18	34	0·390 ± 0·013
(7) Maximum efflux rate (m-mole ^{24}Na (kg cell fluid)$^{-1}$ min^{-1})	15	31	10·4 ± 0·55
(8) Apparent rate constant for extracellular clearance, k_b (min^{-1}):			
from eqn. (10)	18	34	0·83 ± 0·04
from eqn. (13)	18	34	1·16 ± 0·09

to reduce variation between ganglia. Fig. 8 shows an Arrhenius plot relating the logarithm of this fractional rate constant against the reciprocal of the stimulating temperature in °K. The points fit two lines intersecting at 20° C. The apparent activation energies (E_s) for the two segments were measured from the slopes using the modified Arrhenius equation

$$\log (k_2/k_1) = \frac{E_s}{2{\cdot}303R}\left[\frac{1}{T_2} - \frac{1}{T_1}\right], \qquad (14)$$

where k_1 and k_2 are the rate constants at T_1 and T_2 °K and R is the gas constant. The apparent activation energies were 31·2 kcal. mole^{-1}

(< 20° C) and 8·0 kcal. mole^{-1} (> 20° C). The rate constant for the electrogenic effect of Na extrusion (Brown *et al.* 1972; superimposed triangles in Fig. 8) showed a rather similar temperature dependence, though the demarcation at 20° C appeared less abrupt.

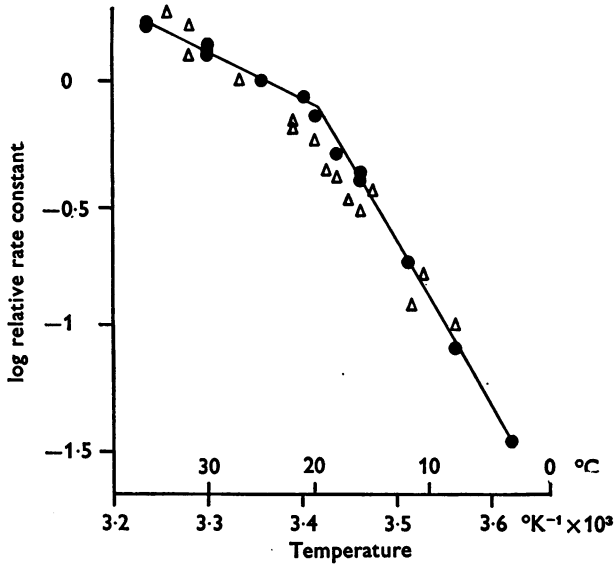

Fig. 8. Arrhenius plot of *log* maximum rate constant (ordinate) against the reciprocal of the absolute temperature (T^{-1}, °K; abscissa) for temperature activated ^{24}Na efflux (○, present experiments) and post-carbachol hyperpolarization (△, recalculated and transposed from Fig. 6 of Brown *et al.* 1972). Each point (●) represents a measurement from a single efflux 'run', except at 3° C which gives the mean from twenty-four ganglia before warming. Points at other temperatures were obtained from experiments on five different ganglia. In each experiment the maximum rate constant (k^C_{max}) attained at each stimulation temperature was expressed as a proportion of that attained in the same experiment at 25° C, to reduce variation between different ganglia: ordinates give this relative rate constant.

The low activation energy above 20° C might suggest that some diffusional process becomes rate-limiting at high temperature, such as the supply of metabolic substrate or external K. This should produce a cut-off in the actual *rate* of ^{24}Na extrusion, rather than the rate *constant*, which was not observed in practice. As indicated in Fig. 3, restricted extracellular clearance rates of extruded ^{24}Na will tend to reduce the apparent rate constant measured after short efflux times as the true rate constant increases, by perhaps 10 % or so. However, this will be a progressive effect, and would not of itself explain the sharp break in the Arrhenius plot, though it might lead to some underestimate of the activation energy at high temperatures.

Inflexions at 20° C have also been noted in Arrhenius plots for (Na + K) – activated ATPase from rat brain (Gruener & Avi-Dor, 1966) and rabbit kidney (Charnock, Cook & Casey, 1971). Activation energies reported in these studies were (> and < 20° C): 7·8 and 19·1 and 13·5 and 28·5 kcal. mole^{-1} respectively. This suggests

that the biphasic Arrhenius plot observed in the present experiments may indeed reflect some fundamental property of the Na-transport mechanism *per se*. Recent observations using spin-label techniques (Grisham & Barnett, 1973) have led to the conclusion that the discontinuity results from a transition in the state of fluidity of the associated membrane lipids, presumably affecting the ability of the ATPase/carrier complex to undergo the rotational or conformational changes necessary for effective transport.

Effect of external K concentration on ^{24}Na efflux

When K was omitted from the surrounding medium ($[K]_e = 0$) the maximum rate constant k^C attained during temperature-stimulated ^{24}Na efflux was reduced to 38 ± 2 % (mean ± S.E. of mean of eight determinations) of that observed in normal Krebs solution ($[K]_e = 6$ mM). With prolonged exposure to 0-$[K]_e$ solution the rate constant declined further, though to a variable extent. Restoration of 6 mM-$[K]_e$ after a period of 0-$[K]_e$ solution accelerated the efflux rate, though not always to the full rate constant originally attained during continued efflux in 6 mM-$[K]_e$.

A further exploration of the change in temperature-stimulated extrusion rate constant with external K concentration over the range 0–20 mM-$[K]_e$ is shown in Fig. 9. As with temperature studies, the maximum rate constant attained at each K concentration was expressed as a fraction (f) of that obtained in normal Krebs solution ($[K]_e = 6$ mM), to reduce variation between different ganglia. After subtraction of the residual rate constant in K-free solution, the K-sensitive component of ^{24}Na efflux, as represented by the corrected fractional rate constant f', showed an approximately hyperbolic relationship to $[K]_e$ (represented by the smooth curve in Fig. 9), such that:

$$f' = \frac{f'_{max}[K]_e}{\phi + [K]_e}, \tag{15}$$

where ϕ is a constant equal to the half-saturation value for $[K]_e$ (i.e. to the apparent Michaelis constant K_m). A double reciprocal (Lineweaver-Burk) plot of f'^{-1} versus $[K]_e^{-1}$ (inset, Fig. 9) was linear over the range 3–20 mM-$[K]_e$, from which values for ϕ of 5·6 mM-$[K]_e$ and f'_{max} of 1·99 could be deduced. The latter corresponds to an uncorrected maximum rate constant k^C of 0·58 min^{-1} (k^C at 6 mM-$[K]_e$ being $0{\cdot}36 \pm 0{\cdot}02$ min^{-1} in these experiments).

The rate constant for ^{24}Na extrusion in nominally K-free solution was appreciably higher than that at low temperatures or in the presence of ouabain (see Table 2). One reason for this might be residual exchange diffusion of ^{24}Na for unlabelled extracellular Na: this is considered further elsewhere. A second problem is that the interstitial K concentration is unlikely to be zero in nominally K-free solution, because of leakage of intracellular K (Harris & Burn, 1949; Keynes, 1954). The rate constant for ^{42}K efflux from isolated ganglia is 0·017 min^{-1} at 25° C (C. N. Scholfield, unpublished observations; Harris & McLennan (1953) and Brinley (1967) give compatible values at other temperatures), while $[K]_i$ at the time of temperature stimulation

(i.e. after 4 min loading plus 15 min cold wash in K-free solution) might be around 160 mM (Brown & Scholfield, 1974). Assuming an effective rate constant for the extracellular clearance of K similar to that for extracellular ^{24}Na wash out (about 0·8 min^{-1}, this paper) and an extracellular space equal to the intracellular volume (Brown, Halliwell & Scholfield, 1971), and neglecting re-uptake by the Na/K exchange pump, eqn. (6) suggests a maximum interstitial K concentration of 3·2 mM after 5 min washing at 25° C, declining to 2·5 mM after 20 min. This would produce appreciable Na-pump stimulation.

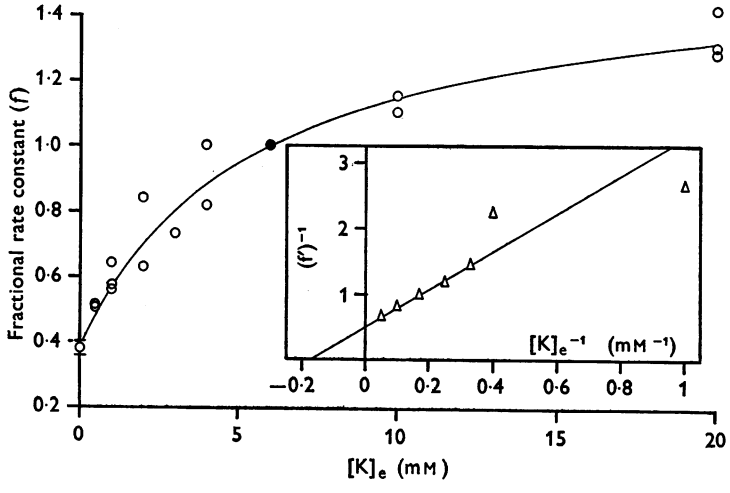

Fig. 9. Effect of changing the concentration of K in the effluent medium ($[K]_e$) on the rate constant for temperature-stimulated ^{24}Na extrusion measured at 25° C. Ordinates: maximum rate constant k^C_{max}, normalized to that observed in 6 mM $[K]_e$ ($=f$, see text). Abscissa: K concentration in the effluent medium. Each point represents a single efflux 'run' determination; points are aggregated from five experiments on five ganglia. The line is drawn according to the hyperbolic text-eqn. (16) with ϕ = 5·6 mM-$[K]_e$. *Inset*: Lineweaver-Burk plot of the K-sensitive component of ^{24}Na efflux. Ordinates: reciprocal of the fractional rate constant f' defined by text-eqn. (15) with $f' = 0$ when the normalized rate constant f = 0·38, and $f' = 1$ when $f = 1$. Abscissa: reciprocal of $[K]_e$. The line is drawn by eye.

This source of Na-pump stimulation should diminish following more prolonged exposure to K-free solution. Some further reduction in the rate constant to 0·1 min^{-1} or less was observed after 20–25 min in K-free solution, but this could also relate to the fade observed in normal solution with prolonged washing (see Methods). In three ganglia immersed in K-free solution for 2–4 hr before loading the maximum rate constants subsequently attained on temperature-stimulation (also in K-free solution) were 24, 29 and 37 % of the control values. This inhibition is slightly greater than that obtained without pre-incubation but is rather disappointing for a totally K-dependent extrusion process since interstitial [K] predicted from eqn. (6) should be then less than 0·5 mM.

K substituents. Substitution of 6 mM-$[Cs]_e$ for 6 mM-$[K]_e$ reduced the rate constant k^C by 40 and 26 % (two experiments). This is equivalent to

reducing $[K]_e$ to 1·2 and 2·4 mM, respectively, a relative activity comparable with that observed for support of post-carbachol hyperpolarization (Brown *et al.* 1972). Li appeared to substitute weakly for K, for replacement of Na by Li (143 mM) raised the efflux rate in K-free solution to that observed in normal Krebs solution (see Table 3 below). It may be that external Na normally inhibits K activation of Na extrusion to some extent and that this effect is not shared by Li, as suggested by Baker & Connelly (1966).

Effect of Na-pump inhibitors

Table 2 shows the results of some tests with chemical inhibitors of active Na extrusion. Cyanide (2 mM), DNP (1 mM) and ouabain (up to 1·4 mM) reduced the rate constant for temperature-stimulated ^{24}Na efflux by 50–90 % at 25° C and 6 mM-$[K]_e$. Iodoacetate (2 mM) by itself had little effect but appeared to increase the effect of cyanide and DNP. Ouabain was tested over a wider concentration range and exerted a half-maximal effect (i.e. k^C reduced by 45 %) at $\sim$ 60 μM. This is reasonably close to the concentration (40 μM) required for half-maximal reduction of the electrogenic hyperpolarization (Brown *et al.* 1972). The rate constant increased again on removing ouabain (according with the reversibility of its effect on electrogenic Na-pumping: Brown *et al.* 1972) but restoration of the efflux rate was less rapid than that obtained on restoring K or raising the temperature.

Effect of external Na

Exchange diffusion of intracellular ^{24}Na for unlabelled external Na (Ussing, 1949) might contribute to the measured ^{24}Na efflux in Na solution, and in particular to the high residual rates of efflux observed in K-free solution (Garrahan & Glynn, 1967). To test this, external Na was replaced with Li, sucrose or choline (with added hexamethonium to prevent depolarization) in both cold-wash and subsequent temperature-stimulating solutions, and the rate constants attained in these solutions compared with those in normal (143 mM [Na]) solution (Table 3). Removal of external Na did not consistently reduce k^C_{max} attained in either 6 mM-$[K]_e$ or 0 mM-$[K]_e$ solution. On the contrary, replacement of Na by Li in K-free solution restored the rate constant to that attained in normal Krebs solution, as noted above. Addition of 1·4 mM ouabain to K-free solution produced considerable inhibition, and this was increased on further replacing Na with sucrose, but this might well have resulted from a cumulative effect of the ouabain. It was also noted that the kinetics of ^{24}Na efflux in Na solution (as depicted in Figs. 2 and 7) were not substantially altered in form on transferring to Na-free solution, suggesting that isotopic

TABLE 2. Effects of some metabolic inhibitors on the maximum rate constant k^o for ^{24}Na extrusion at 25° C

Inhibitor	Concn. mM	Experiment no.	Rate constant (min^{-1}) Control	Test	Inhibition %
Sodium cyanide	2	30/12/5b	0·376	0·140	63
	2	30/12/6c	0·354	0·236	33
	2	30/12/2b	0·354	0·102	71*
Dinitrophenol	1	1/12/6b	0·367	0·175	52
	1	1/12/6a	0·327	0·179	45
	1	18/11/2	0·354	0·198	44
Cyanide + iodoacetate	2 + 2	21/9/2	0·360	0·156	57
	2 + 2	30/12/6b	0·354	0·067	81*
Dinitrophenol + iodoacetate	1 + 2	18/11/3	0·354	0·073	79
Ouabain	0·0044	3/11/2	0·333	0·325	2
	0·0137	19/10/2	0·353	0·274	23*
	0·044	3/11/4	0·333	0·231	30
	0·137	14/9/2	0·310	0·136	56
	0·137	19/10/4	0·356	0·105	70*
	0·44	3/11/6	0·325	0·067	79
	1·37	14/9/3	0·310	0·064	80
	1·37	19/10/6	0·365	0·044	88*

Inhibitors were added immediately after loading except those marked (*), which were added 10 min before loading with ^{24}Na.

TABLE 3. Effect of replacing external Na with Li, sucrose or choline on the rate constant for ^{24}Na efflux measured at 25° C in the presence of 0 or 6 mM-$[K]_e$.

Experiment	Na substituent	Maximum rate constant k^o (min^{-1}) 0 $[K]_e$	6 $[K]_e$
21/9	Na	0·118	0·383
	Li	0·340	0·348
17/11	Na	0·196	0·352
	Li	0·350	—
24/11	Na	0·175	0·386
	Li	0·357	0·384
1/2	Na	0·303*	0·429
	sucrose	0·259*	0·352
2/2	Na†	0·104*	—
	sucrose†	0·054*	—
8/2	Na	0·169*	0·366
	sucrose	0·240*	—
	choline	0·257*	—

* Preincubated for 2–4 hr in K-free solution.
† Ouabain (1·37 mM) present throughout.

dilution of intracellular ^{24}Na by influent unlabelled Na was not an important determinant of ^{24}Na extrusion kinetics.

Variation of ^{24}Na efflux with different loading conditions

The peak rate constant for ^{24}Na efflux tended to diminish when (*a*) the period of exposure to carbachol – ^{24}Na solution was lengthened, or (*b*) when the concentration of carbachol in the loading solution was increased (Fig. 10). Thus, in two ganglia k^{C}_{max} after loading in 55 μM

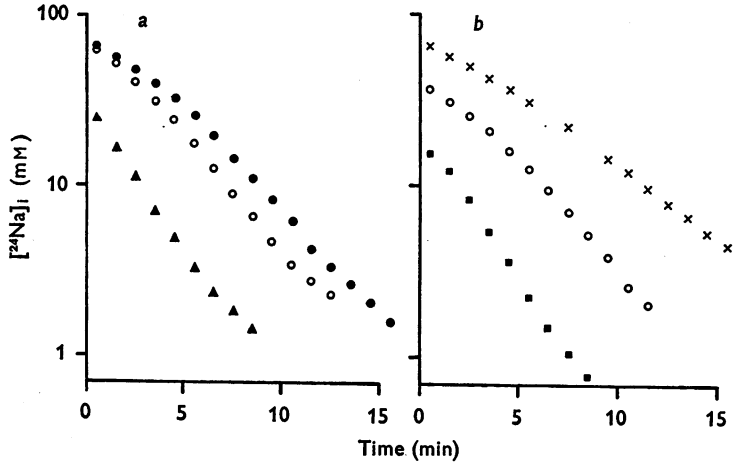

Fig. 10. Effects of (*a*) increasing the duration of the ^{24}Na loading period and (*b*) increasing the concentration of carbachol in the ^{24}Na loading solution on subsequent temperature-stimulated efflux measured at 25° C (two ganglia). Ordinates: intracellular ^{24}Na concentration (m-mole (kg cell fluid)$^{-1}$, see Methods). Abscissae: time after warming, in min. In *a* a ganglion was loaded on different occasions in ^{24}Na solution containing 180 μM carbachol for 2 (▲), 4 (○) and 10 (●) min, then washed for 15 min at 3° C before warming and measuring ^{24}Na efflux. In *b* another ganglion was loaded for 4 min in ^{24}Na solution containing 60 (■), 180 (○) and 600 (×) μM carbachol.

carbachol was 24 and 29 % greater than that attained after loading in the standard concentration of 180 μM; in three ganglia k^{C}_{max} after 550 μM carbachol was 12, 7 and 15 % less than that after 180 μM carbachol. However, this difference did not extend to the extreme situation where ganglia were loaded in carbachol-free solution, in which rate constants quite comparable with those observed after loading in 180 μM carbachol were obtained (see Fig. 1). Changes in k^{C}_{max} of comparable magnitude occurred with variations in loading duration.

Procedures such as increasing the concentration of carbachol in the ^{24}Na solution or lengthening the load-time served to increase the cellular uptake of ^{24}Na. This

raises the possibility that the rate constant for Na extrusion might diminish with increasing $[Na]_i$ – i.e. the extrusion process might saturate with $[Na]_i$ and so not be first-order as demanded by eqn. (1). While this cannot be rigorously excluded two lines of evidence suggest that this is not the sole reason for the variation in maximal rate constant observed in the above experiments. Firstly, it is clear from Fig. 10 (where tissue ^{24}Na is expressed as calculated $[^{24}Na]_i$) that the maximum rate constant was attained at approximately the same intracellular ^{24}Na concentrations (between 4 and 10 mM), which are well below the initial values of $[^{24}Na]_i$. Secondly, the initial values of $[^{24}Na]_i$ obtained in control runs using a constant (180 μM) concentration of carbachol and a constant (4 min) loading time varied between extremes of 24 and 76 mM, with no correlative variation in k^{C}_{max}. A further indication that the efflux kinetics were not strongly dependent upon the absolute value of $[Na]_i$ is provided by the lack of effect of external Na replacement noted above. An alternative explanation for the effect of loading conditions on subsequent efflux rates might be that the *distribution* of ^{24}Na within the tissue was altered. For example (as pointed out in the Appendix) large cells would have a slower efflux rate constant than small cells and would also fill more slowly with ^{24}Na during loading. The effect of more protracted loading or (possibly) increased carbachol concentration could then be to increase the contribution of large cells to the observed efflux and reduce the over-all rate constant.

DISCUSSION

The efflux of ^{24}Na from Na-loaded ganglia produced by temperature stimulation accords with the operation of a Na-extrusion pump qualitatively similar to that studied more thoroughly in other tissues (q.v. Glynn, 1968; Baker, 1972). Thus, the extrusion rate constant showed an acute temperature sensitivity, a saturable dependence upon external [K], and was reduced by ouabain and metabolic inhibitors. No substantial fraction of the ^{24}Na extruded appeared to exchange compulsorily with external Na, to judge from Na-replacement experiments, but it is doubtful whether the condition most likely to favour such exchange (complete absence of external K: Garrahan & Glynn, 1967) could be fully attained.

The anatomical complexity of this tissue hindered a precise description of the kinetics of Na extrusion. Nevertheless, a fairly satisfactory interpretation of the exit of labelled Na could be made by assuming the bulk ($> 95\%$) of the ^{24}Na to be extruded from the cells via first-order kinetics, and making some simple corrections for transit through the extracellular space. First-order kinetics for Na extrusion at elevated internal Na concentrations have been observed in single-neurone preparations (Brinley & Mullins, 1968; Thomas, 1969); and the neurones in the ganglion appear sufficiently homogeneous in anatomical dimensions for such kinetics to be manifest as an exponential decline in ^{24}Na within the total neurone population (see Appendix). However, it appears very probable that, fundamentally, the rate of Na extrusion is a saturable function of some power (probably 3) of internal Na concentration (Keynes & Swan, 1959; Rang & Ritchie, 1968; Garay & Garrahan, 1973). This could account for

our observed deviations from exponential kinetics after prolonged washing, i.e. at low values of $[Na]_i$ as an alternative to the multiple Na pools offered as a formal interpretation in Methods and Appendix. First-order kinetics might then be apparent at elevated levels of $[Na]_i$ if secondary binding sites for Na were saturated.

The rate constant for Na extrusion from sympathetic ganglion cells is high ($\sim 0{\cdot}35\ min^{-1}$ at 25° C) implying an appropriately high energy consumption and oxygen requirement. For example, at rest a steady pumped efflux of about 5·8 m-mole (kg cell fluid)$^{-1}$ min^{-1} may be deduced, necessitating an oxygen consumption rate of 0·13 μmole O_2 (g wet tissue weight)$^{-1}$ min^{-1} at Na: P and $P{:}O$ ratios of 3:1 (Glynn, 1962; Baker & Shaw, 1965; McIlwain, 1966). This is about 42 % of the resting O_2 consumption at 24° C (Larrabee, 1958) (111 μmole (g dry weight)$^{-1}$ hr^{-1} = 0·31 μmole. (g wet weight)$^{-1}$ min^{-1}), a proportion in line with previous calculations in isolated brain tissue (Whittam, 1962; Keesey & Wallgren, 1965). After Na loading in carbachol solution the average peak Na efflux rate would correspond to a maximal oxygen consumption rate of 0·57 μmole (g wet weight)$^{-1}$ min^{-1}. Oxygen consumption following this type of stimulation has not been measured directly, but Dolivo & Larrabee (1958) recorded a rate of 168 μmole (g dry weight)$^{-1}$ hr^{-1} (= 0·47 μmole (g wet weight)$^{-1}$ min^{-1}) at 23° C after repetitive preganglionic nerve stimulation for 2·5 hr at an average rate of 4·6 Hz. Thus, though high, the O_2 requirements of sympathetic ganglia for support of Na extrusion rates observed in the present experiments are compatible with previously-recorded values.

We have previously noted that sympathetic ganglia exposed to nicotinic depolarizing agents show a pronounced hyperpolarization on washing out the depolarizing agent, and have attributed this to an electrogenic effect of the Na-pump (Brown *et al.* 1972). The present observations are compatible with this interpretation, in that the rate constant, K sensitivity, temperature sensitivity and response to inhibitors are closely similar for the two processes. Further, temperature stimulation also generated a hyperpolarization whose time course showed a fair approximation to that of the extrusion of ^{24}Na (see Fig. 7). Some estimate of the magnitude of the electrogenic effect may be obtained from the ^{24}Na efflux measurements if one assumes that a fixed proportion of Na is extruded electrogenically (probably one third: Thomas, 1969), which seems plausible from Fig. 7. The peak rate of ^{24}Na extrusion (10·4 m-mole (kg cell fluid^{-1} min^{-1}, Table 1), when adjusted for the attenuation by extracellular clearance and the specific activity of the intracellular ^{24}Na, corresponds to about 24 m-mole, (kg cell fluid)$^{-1}$ min^{-1} total Na extrusion. Assuming (i) a total intracellular volume of $\sim 0{\cdot}5\ \mu l.$ per ganglion (Brown & Scholfield, 1974 and Table 1), (ii) between 10,000 and 30,000 neurones per ganglion (per-

sonal observation), (iii) a coupling ratio of 3 Na:2 K (Thomas, 1969), and (iv) a cell membrane resistance of 60–80 MΩ (Perri, Sacchi & Casella, 1970; Adams & Brown, 1973 and unpublished observations), the Na current would produce an electrogenic hyperpolarization of somewhere between 15 and 60 mV. This appears an appropriate order of magnitude to account for the post-carbachol hyperpolarization (up to 5 mV observed with extracellular electrodes; Brown *et al.* 1972). Such an electrogenic effect is likely in any neurone where the extrusion rate is sufficiently rapid and the membrane resistance is high because of the inherently non-neutral nature of the Na pump (Kerkut & York, 1971; Thomas, 1972). In this respect, the ganglionic Na-pump does not appear at all unusual. Nevertheless, special interest attaches to electrogenic hyperpolarization in ganglion cells as a possible cause of transmission and drug-induced after-potentials and inhibition (see, for example, Koketsu, 1969). The experiments described in this paper may assist further study of such effects by providing a basis for direct measurements of changes in Na-extrusion rates.

This investigation was aided by a grant from the American Medical Association Education and Research Foundation. We thank Dr Jane A. C. Young and Miss Susan Lemmon for histological assistance.

APPENDIX

Effect of ganglion cell size on the kinetics of ^{24}Na efflux

Desaturation curves for ^{24}Na loss departed appreciably from a simple exponential following prolonged washing (e.g. Fig. 2). As suggested in Methods, this might result from a heterogeneous distribution of intracellular ^{24}Na with respect to efflux rate constant. In this Appendix we consider whether, if each ganglion cell is considered as a separate compartment, such deviations might arise simply from variation in the physical dimensions of the cells. In this we follow Zierler's (1966) theoretical treatment for muscle cells, adapting this for ganglion cells, and attempt some prediction of efflux curves using information on the distribution of ganglion cell dimensions as revealed by histological examination.

The starting assumption for this treatment is that the rate of Na extrusion (m) per cell is directly proportional to the intracellular Na concentration C, and the surface area of cell membrane A:

$$m = \alpha CA, \tag{i}$$

where α is a 'transfer coefficient' equivalent to a permeability coefficient (cf. Harris & Burn, 1949; Keynes & Lewis, 1951). This transfer coefficient for active transport might depend upon the density and turnover number of carrier sites. If these are constant in different cells, the rate constant for any one cell as defined in text-eqn. (1) becomes proportional to the

surface area/volume ratio. Assuming the ganglion cells to be spherical with radius r the rate constant is defined as:

$$k = 3 \alpha r^{-1}. \tag{ii}$$

The initial ^{24}Na content of a cell (a_0 in text-eqn (1)) is given by the product of the initial concentration (C_0) and the cell volume:

$$a_0 = 4/3 \pi r^3 C_0. \tag{iii}$$

At equilibrium C_0 will be the same for all cells, and will be equal to the equilibrium concentration C_{eq}. With short (non-equilibrium) loading conditions C_0 might be considered to approach C_{eq} exponentially with loading time t_L as:

$$C_0 = C_{eq} [1 - \exp(-3\beta t_L r^{-1})], \tag{iv}$$

where β is an (inward) passive permeability coefficient (cf. Zierler, 1966). Translating from total Na to ^{24}Na (i.e. assuming isotopic dilution to have no effect on kinetics) expressions (ii) and (iii) may be substituted in text-eqn. (1) (Methods) to give the ^{24}Na content of a cell after efflux time t as:

$$a_t = 4/2 \pi r^3 C_0 \exp(-3 \alpha t r^{-1}) \tag{v}$$

and the corresponding efflux rate (text-eqn. (2)) as

$$m_t = 4 \pi r^2 \alpha C_0 \exp(-3 \alpha t r^{-1}). \tag{vi}$$

Values for cell radii were obtained from histological sections of three ganglia. The ganglia were isolated, desheathed and maintained in oxygenated Krebs solution at 25° C for some hours as described in Methods, and then fixed in 2·5 % glutaraldehyde buffered to pH 6·8 with 0·095 M phosphate buffer. After dehydration, the ganglia were embedded in paraffin wax and serial sections cut at 5 μm thickness, mounted and stained with toluidine blue. In each twentieth section the diameters of all neurones sectioned meridionally (i.e. through the nucleus) were measured in two directions (horizontally and vertically) to the nearest 2·5 μm using a calibrated eyepiece grid at × 1000 magnification. From individual histograms relating occurrence frequency against cell diameter, the average frequency curve shown in Fig. 11 was determined, in which cell radii are expressed as a fraction of the average modal radius (r_m) of the cells in the three ganglia. Though skewed, the distribution appears unimodal, with 95 % of the cell diameters falling within the range 0·51–1·71 r_m.

The initial ^{24}Na content of each group of cells represented by the individual histogram-blocks in Fig. 11 was calculated as a fraction of the total intracellular ^{24}Na in the ganglion from equations (iii) and (iv) under conditions of equilibrium and non-equilibrium loading respectively. For the latter the loading time t_L was taken as equivalent to one influx time constant for the modal cell group ($\tau_m = 3\beta_m^{-1}$) from uptake data in

Fig. 4*b*. The fractional ^{24}Na contents of each cell group are superimposed in Fig. 11. The larger cells clearly contain an amount of ^{24}Na disproportionately great compared with their numbers: the effective modal radius with respect to initial ^{24}Na content is $1{\cdot}21r_m$, after equilibrium loading and $1{\cdot}18r_m$ after non-equilibrium loading.

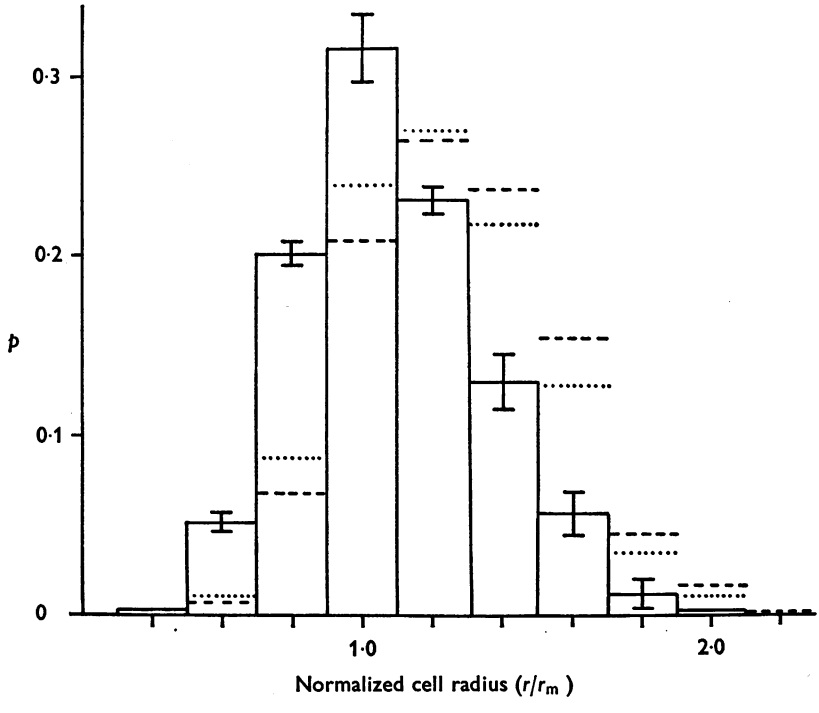

Fig. 11. Distribution of cell radii in rat superior cervical ganglia. Ordinates: proportion of total cells counted (p). Abscissa: cell radius expressed as a fraction of the mean modal radius (r_m). Data was obtained from three ganglia (2328 neurones measured). The height of each solid block represents the mean from three ganglia; vertical show bars S.E. of means. The initial ^{24}Na contents of each cell group, calculated from eqns. (iii) and (iv) after loading to equilibrium ($t_L = \infty$, ----) and to one modal influx time constant ($t_L = 3\beta^{-1}$, ...), and expressed as a fraction of the total ^{24}Na content of all the cells, are superimposed.

Theoretical desaturation and efflux curves for the whole ganglion were calculated by applying eqns. (v) and (vi) to each histogram block in Fig. 11, summing and adjusting to unity total initial content. Calculated curves extending over 8 efflux time constants (τ_m) for the modal cell group are shown in Fig. 12. The curves are not single exponentials, as shown by the diminishing rate constant in Fig. 12*c*, but approximate quite closely thereto. The apparent overall rate constant (k_{app}) is less than that of the

modal cells (k_m) throughout. Maximally (at $t = 0$) $k_{app} = 0{\cdot}82\, k_m$; this corresponds to the rate constant of a cell of radius $1{\cdot}22 r_m$. After eight time constants $k_{app} = 0{\cdot}65\, k_m$, corresponding to an apparent cell radius of

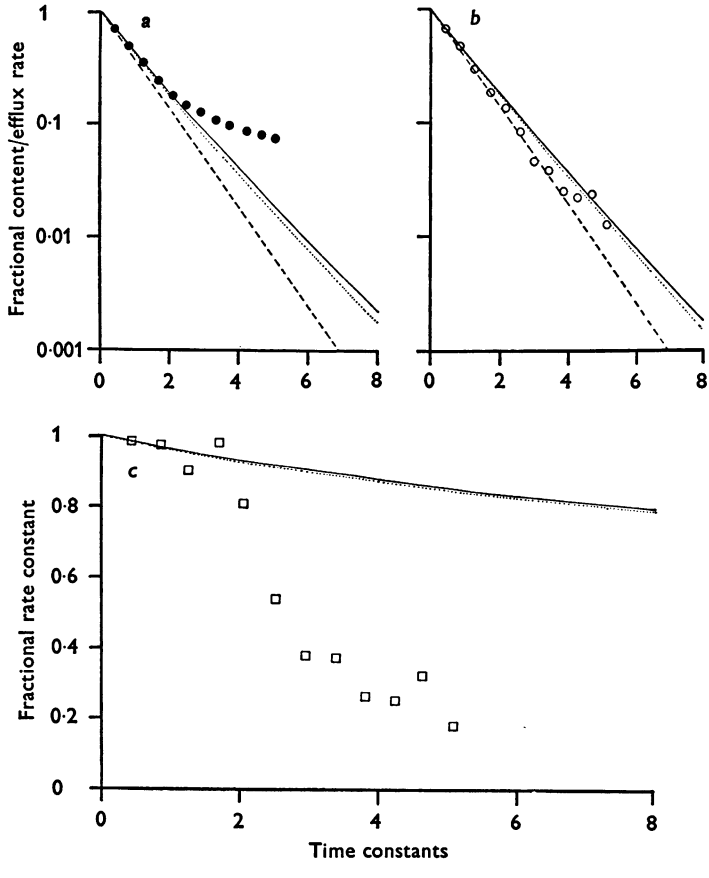

Fig. 12. Hypothetical ^{24}Na efflux curves calculated from the distribution of cell diameters in Fig. 11 according to Appendix eqns. (v) and (vi), assuming (i) loading to equilibrium (——) and (ii) loading for one influx time constant of the modal cell population (.....). Graph *a* shows the decline in total ^{24}Na content (eqn. (v)) and *b* shows the efflux rate (eqn. (vi)) both expressed as a fraction of that obtaining at zero efflux time; the interrupted line shows the expected result for a uniform population of cells with the diameter of the modal cell group, on the same scale. Graph *c* shows the change in rate constant with time, calculated by dividing eqn. (v) and (vi) and expressed as a fraction of the initial rate constant. The time scale is expressed as multiples of the time constants for the efflux from the modal cell population (τ_m). Superimposed points are derived from Fig. 2, the data being converted to the same time scale by assuming the maximum observed rate constant to be 0·82 times that of the modal cell population.

$1{\cdot}54\,r_m$. Thus, there is a trend with time towards a more dominant contribution by the larger cells to the measured efflux and a corresponding fall in the measured rate constant.

For comparison with these theoretical curves experimental data derived from Fig. 2 are superimposed on the curves in Fig. 12. The transposition was made by taking experimental points from the time of peak rate constant onwards (from 6 min in Fig. 2). setting this time as 0 and the observed k^C_{max} at this time as $0{\cdot}82\,r_m$ as above, so allowing conversion of time scales and rate constants. Predicted and observed values accord well up to $2\tau_m$ (i.e. to about 5 min real efflux time), suggesting that the small (10% or so) diminution in the observed rate constant at this time could be attributed solely to the normal distribution of cell diameters. However, the more marked decline in rate constant with further washing could not be so explained, since it would require the presence of some neurones in the ganglion with a radius at least six times the modal radius (some 80 μm or more), for which there is no histological evidence. This would support the concept of a subsidiary, more slowly exchanging pool of intracellular ^{24}Na as represented in text-eqn. (11). Among several possibilities may be suggested (*a*) entry of ^{24}Na into some neurones with an unusually slow rate of Na pumping, resulting from metabolic or carrier deficiency, or into other elements (? glia) with low pump rates, or (*b*) fractionation of accumulated ^{24}Na such that a proportion is 'bound' or restricted in terms of access to pump sites. Alternatively, the assumed kinetics may be an oversimplification at low internal Na concentrations, as considered in Discussion.

REFERENCES

ADAMS, P. R. & BROWN, D. A. (1973). Action of γ-aminobutyric acid (GABA) on rat sympathetic ganglion cells. *Br. J. Pharmac.* **47**, 639–640*P*.

ATKINS, G. L. (1969). In *Multicompartment Models for Biological Systems*, p. 29. London: Methuen.

BAKER, P. F. (1972). The sodium pump in animal tissues and its role in the control of cellular metabolism and function. In *Metabolic Pathways*, vol. VI, ed. HOKIN, L. E. pp. 243–268. New York: Academic Press.

BAKER, P. F. & CONNELLY, C. M. (1966). Some properties of the external activation site of the sodium pump in crab nerve. *J. Physiol.* **185**, 270–297.

BAKER, P. F. & SHAW, T. I. (1965). A comparison of the phosphorus metabolism of intact squid nerve with that of the isolated axoplasm and sheath. *J. Physiol.* **180**, 424–438.

BITTAR, E. E. (1971). An investigation of Na efflux from the toad oocyte using cold shock as a technique. *Experientia* **27**, 268–270.

BOSTEELS, S. & CARMELIET, E. (1972). Estimation of the intracellular Na concentration and transmembrane Na flux in cardiac Purkinje fibres. *Pflügers Arch. ges. Physiol.* **336**, 35–47.

BRINLEY, F. J., JR. (1963). Ion fluxes in the central nervous system. *Int. Rev. Neurobiol.* **5**, 183–241.

BRINLEY, F. J., JR. (1967). Potassium accumulation and transport in the rat sympathetic ganglion. *J. Neurophysiol.* **30**, 1531–1560.

BRINLEY, F. J., JR. & MULLINS, L. J. (1968). Sodium fluxes in internally dialysed squid axons. *J. gen. Physiol.* **52**, 181–211.

BROWN, D. A., BROWNSTEIN, M. J. & SCHOLFIELD, C. N. (1969). On the nature of the drug-induced after-hyperpolarization in isolated rat ganglia. *Br. J. Pharmac.* **40**, 559–561*P*.

BROWN, D. A., BROWNSTEIN, M. J. & SCHOLFIELD, C. N. (1972). Origin of the after-hyperpolarization that follows removal of depolarizing agents from the isolated superior cervical ganglion of the rat. *Br. J. Pharmac.* **44**, 651–671.

BROWN, D. A., HALLIWELL, J. V. & SCHOLFIELD, C. N. (1971). Uptake of nicotine and extracellular space markers by isolated ganglia in relation to receptor activation. *Br. J. Pharmac.* **42**, 100–113.

BROWN, D. A. & SCHOLFIELD, C. N. (1974). Changes of intracellular sodium and potassium ion concentration in isolated rat superior cervical ganglia induced by depolarizing agents. *J. Physiol.* **242**, 307–319.

CHARNOCK, J. S., COOK, D. A. & CASEY, R. (1971). The role of cations and other factors on the apparent energy of activation of (Na+K)-ATPase. *Archs Biochem. Biophys.* **147**, 323–329.

DOLIVO, M. & LARRABEE, M. G. (1958). Metabolism of glucose and oxygen in a mammalian sympathetic ganglion at reduced temperature and varied pH. *J. Neurochem.* **3**, 72–88.

GARAY, R. P. & GARRAHAN, P. J. (1973). The interaction of sodium and potassium with the sodium pump in red cells. *J. Physiol.* **231**, 297–325.

GARRAHAN, P. J. & GLYNN, I. M. (1967). The behaviour of the sodium pump in red cells in the absence of external potassium. *J. Physiol.* **192**, 159–174.

GLYNN, I. M. (1962). Activation of adenosinetriphosphatase activity in a cell membrane by external potassium and internal sodium. *J. Physiol.* **160**, 18–19*P*.

GLYNN, I. M. (1968). Membrane ATPase and cation transport. *Br. med. Bull.* **24**, 165–169.

GRISHAM, C. M. & BARNETT, R. E. (1973). The role of lipid-phase transitions in the regulation of the (sodium+potassium) adenosine triphosphatase. *Biochemistry, N.Y.* **12**, 2635–2637.

GRUENER, N. & AVI-DOR, Y. (1966). Temperature-dependence of activation and inhibition of rat-brain adenosine triphosphatase activated by sodium and potassium ions. *Biochem. J.* **100**, 762–767.

HARRIS, E. J. (1972). *Transport and Accumulation in Biological Systems*, 3rd edn., p. 38. London: Butterworths.

HARRIS, E. J. & BURN, G. P. (1949). The transfer of sodium and potassium ions between muscle and the surrounding medium. *Trans. Faraday Soc.* **45**, 508–528.

HARRIS, E. J. & MCLENNAN, H. (1953). Cation exchanges in sympathetic ganglia. *J. Physiol.* **121**, 629–637.

HUXLEY, A. F. (1960). Appendix to Solomon, A. K. (1960). *Mineral Metabolism*, ed. COMAR, C. L. & BRONNER, F., vol. 1A, pp. 163–166.

KEESEY, J. C. & WALLGREN, H. (1965). Movements of radioactive sodium in cerebral cortex slices in response to electrical stimulation. *Biochem. J.* **95**, 301–310.

KERKUT, G. A. & YORK, B. (1971). *The Electrogenic Sodium Pump*. Bristol: Scientechnica.

KEYNES, R. D. (1954). The ionic fluxes in frog muscle. *Proc. R. Soc.* B. **142**, 359–382.

KEYNES, R. D. & LEWIS, P. R. (1951). The resting exchange of radioactive potassium in crab nerve. *J. Physiol.* **113**, 73–98.

KEYNES, R. D. & SWAN, R. C. (1959). The effect of external sodium concentrations on the sodium fluxes in frog skeletal muscle. *J. Physiol.* **147**, 591–625.

KOKETSU, K. (1969). Cholinergic synaptic potentials and the underlying synaptic mechanisms. *Fedn Proc.* **28**, 101–112.

KOSTERLITZ, H. W., LEES, G. M. & WALLIS, D. I. (1968). Resting and acting potentials recorded by the sucrose gap method in the superior cervical ganglion of the rabbit. *J. Physiol.* **195**, 39–53.

KOSTERLITZ, H. W., LEES, G. M. & WALLIS, D. I. (1970). Further evidence for an electrogenic sodium pump in a mammalian sympathetic ganglion. *Br. J. Pharmac.* **38**, 464–465*P*.

LARRABEE, M. G. (1958). Oxygen consumption of excised ganglia at rest and in activity. *J. Neurochem.* **2**, 81–101.

MCILWAIN, H. (1966). *Biochemistry and the Central Nervous System*, 3rd edn., p. 118. London: Churchill.

PERRI, V., SACCHI, O. & CASELLA, C. (1970). Electrical properties and synaptic connections of the sympathetic neurones in the rat and guinea-pig superior cervical ganglion. *Pflügers Arch. ges. Physiol.* **314**, 4–54.

PERSOFF, D. A. (1960). A comparison of methods for measuring efflux of labelled potassium from rabbit atria. *J. Physiol.* **152**, 354–366.

RANG, H. P. & RITCHIE, J. M. (1968). On the electrogenic sodium pump in mammalian nonmyelinated nerve fibres and its activation by various external cations. *J. Physiol.* **196**, 183–221.

TEORELL, H. (1937). Kinetics of distribution of substances administered to the body. *Archs int. Pharmacodyn. Thér.* **57**, 205–225.

THOMAS, R. C. (1969). Membrane currents and intracellular sodium changes in a snail neurone during extrusion of injected sodium. *J. Physiol.* **201**, 495–514.

THOMAS, R. C. (1972). Electrogenic Sodium Pump in Nerve and Muscle cells. *Physiol. Rev.* **52**, 563–594.

USSING, H. H. (1949). Transport of ions across cellular membranes *Physiol. Rev.* **29**, 127–155.

WEAST, R. C. (1971). *Handbook of Chemistry and Physics*, 52nd edn. Table F. 47. Ohio: The Chemical Rubber Co.

WHITTAM, R. (1962). The dependence of the respiration of brain cortex on active cation transport. *Biochem. J.* **82**, 205–212.

ZIERLER, K. Ł. (1966). Interpretation of tracer washout curves from a population of muscle fibres. *J. gen. Physiol.* **49**, 423–431.